RPN5

Radiation Production Notes
Note 5

30 Dec 1968

Generation and Transport of Electron Beams of ν/γ Greater than Unity

by
Thomas H. Storr
Atomic Weapons Research Establishment

First Printed as SSWA/THS/6812/107

1. Introduction

This paper deals with work done at AWRE up to the present time on the production of electron beams of $v/\gamma > 1$, the main object of which is the rapid deposition of electron energy within a variety of sample materials. The electron voltage to be used is to some extent predetermined by the energy-depth profile required in the sample; so that high energy levels are to be obtained primarily by the use of large beam currents, and hence high v/γ . Intended beam parameters for the present work are nominally ~ 100 kA at ~ 1 MV, giving $v/\gamma \sim 2$. The heading of 'generation' of a beam involves primarily the design of a suitable diode cathode-anode combination, and that of 'transport' involves the investigation into conditions necessary for the stable and efficient propagation of a beam beyond the diode. Albeit on a limited scale, more work has so far been devoted to the former category than the latter.

1.1 Drive generators

Two impulse generators have been used, the output parameters of which are listed in Table I. MINI 'B' is an oil-dielectric Blumlein generator using an oil high speed switch and charged by a 40 kJ Marx pulser; it delivers in advance of its main pulse a prepulse of complex waveform with amplitude of ~ 7% of the Blumlein charging level. SPLATTLET is a water-dielectric single coaxial line generator using a water gap output switch and charged by the 90 kJ MOGUL Marx pulser. Its prepulse is an attenuated replica of the line charging waveform whose amplitude, in the absence of a prepulse isolating switch, amounts to around 10% of the line charge level. The effect of the presence and character of a prepulse upon the performance of the electron tube cathode has not been fully determined but it is considered to be of crucial importance.

1.2 Diagnostics

Table I shows the range of diagnostic measurements used with the generators so far, the techniques and apparatus being the same as is described in paper SSWA/MJG/6812/106.[1] The output voltage measurement on MINI 'B' is isolated from the diode section by the substantial electrode inductance, so that it is not accurately possible to derive from this and the current measurement a value for diode impedance as a function of time. Thus the diode impedance considered in the MINI 'B' work is that obtaining at the end of the 50 ns pulse.

The X-ray pinhole camera provides a powerful check on the spatial distribution of the current incident upon a target and, moreover, gives a clear indication of the presence of spurious emission in the diode. The target has for the most part taken the form of a block of carbon, used simultaneously as a single-cell calorimeter with the thermocouple, to determine the total

1. Radiation Production Note 6

TABLE I

	MINI 'B'	SPLATTLET
Output impedance	16 Ω	6 Ω
Pulse duration	50 ns	100 ns
Switched rise time	7 ns	~ 20 ns
Short circuit current rise time	23 ns	~ 25 ns
Tube inductance	~ 300 nH	~ 50 nH
Voltage and current ranges in work on $v/\gamma > 1$ so far:-		
Peak tube voltage	0.5-1.5 MV	0.3-1.0 MV
Peak tube current	50-130 kA	30-130 kA
Diagnostics:-		
Output voltage v. time	✓	✓
Tube current v. time	✓	-
X-ray flux v. time	On few shots	-
Pinhole X-ray camera	✓	✓
Integrated dose (T.L.D.)	✓	✓
Calorimeter target	✓	✓

energy deposition. In shots where an energy measurement was not attempted, the target has taken the form of a foil of tantalum of about 0.003 inches thickness.

2. Generation of Beams

The immediate aims of the cathode development programme started on MINI 'B' were twofold. There was needed (a) a cathode with good overall uniformity of emission at low current density, with electron trajectories paraxial or slowly convergent, for use with a foil anode window as a launcher for beam propagation studies. The low current density requires the use of high aspect ratio parallel-plane geometry in the diode which would minimize damage to the anode foil. Also necessary was (b) a cathode capable of most efficiently concentrating the energy available from the pulser into a small, and if possible adjustable, target area on axis with the greatest uniformity possible; the target could be either in the anode plane or beyond it, providing that the electron trajectories be not too strongly convergent. In view of the likelihood of disruption of the target, the cathode should be robust and easily cleaned.

2.1 Cathode design

The design of the emitting surface in the diode was initially based on work originally done at higher impedance levels, i.e. $\nu/\gamma < 1$. However, it was to be expected that at high ν/γ the effects of self-neutralisation of the beam might be unavoidable at some time during the pulse; here the large self-generated magnetic field becomes dominant and it would be anticipated that the type of pinch phenomena of magnetic origin which have been observed in low ν/γ work would be considerably enhanced. The initial search, therefore, was for a cathode with very uniform emission characteristics over large areas; this eliminated to a large measure any cathode whose operation depends on strong geometrical field enhancement, such as a needle, ball or razor edge. A multiple-needle cathode (using a piece of file cleaning brush pad) showed unstable and non-uniform emission characteristics, as did cathodes comprising inserts of carbon, the object of which was to provide a stabilising resistive backing to the emission surface. Other cathodes investigated were all variants of the plasma cathode in which localised field emission from an insulator-metal combination results in lateral electric fields sufficient to precipitate avalanche breakdown and subsequent growth of a plasma across the insulator, which then operates as a field emitter of virtually zero work function. The most promising emission surface appeared to be an epoxy-filled aluminium honeycomb, described in paper SSWA/MJG/6812/106;[2] this is the logical extension of the multispot type of cathode in which the presence of the aluminium foil throughout the emitting area is intended to ensure the growth of a uniform plasma. Although this type has functioned well at low ν/γ and was the best of the initial selection tried, still further subdivision of the emitting surface appears to be necessary to retain stability of emission at $\nu/\gamma \sim 2$. Three types of honeycomb cathode have so far evolved which are here described individually.

2.2 Plane disc honeycomb cathode

The plane disc cathode comprises a circular disc of epoxy honeycomb 1 cm thick inset into the cathode electrode surface, turned flush and rough polished, as Fig. 1. Two sizes were made, 4.5 cm and 9 cm in diameter. Performance at approximately 1 MV and 100 kA is erratic; although the perveance is higher than that given for space charge-limited emission by the Child-Langmuir relation it is lower than other cathode types and emission does not appear to be proportional to area. The hypothesis to be drawn from this is that emission is not distributed over the whole cathode surface. X-ray pinhole data shows that emission is rarely uniform, but is asymmetrical and tends to collapse in striae or small patches. Such collapse results in blow up of the anode, debris from which damages the cathode surface badly.

2. Radiation Production Note 6

2.3 Annular honeycomb cathode

Several considerations led from the plane disc to the annular cathode, namely (1) the centre area is the part most affected by anode or target debris; (2) the central area is not necessarily the main origin of electrons which are involved in collapse into central spots on the anode, but on the hypothesis that an annular area can be arranged to emit uniformly the removal of a central emitter provides an inner boundary to the current sheet which initially encloses no current, and is therefore not at first subject to self-magnetic collapse towards the axis; (3) by contouring the cathode surface and possibly also the anode surface it is possible to arrange the direction of the accelerating field so as to oppose the self-magnetic forces on electrons in their passage across the diode, such that all electron trajectories are close to being paraxial at the anode surface.

Two annular cathodes have been made and tried (see Fig. 2) and over a limited number of shots have given higher perveance figures than the plane disc cathode. This could be only an apparent effect, the loss of the central area of honeycomb having decreased cathode area without much loss of emission, thus decreasing the normalised resistance $Z\,V^{1/2}\gamma^2/S^2$. So far no clear check has been made of the relation between emission and area; the small annulus has only been tried on MINI 'B', the large on SPLATTLET - their normalised perveances are drastically and unexpectedly different. A possible explanation for this difference may lie in the different nature of the prepulse in the two machines; experiments to investigate the dependence of plasma cathode performance on prepulse are just beginning, since the installation in SPLATTLET of a prepulse isolation switch ahead of the tube. Figs. 3, 4 and 5 show X-ray pinhole photographs and shot data for various electrode geometries using annular cathodes. Emission appears reasonably consistent (shot to shot) and symmetrical. There appears a fairly clear distinction on pinhole data between near-paraxial emission (giving an annular image on the anode) and convergent current contributing to a central core. A hypothesis is that the first occurs early in the pulse, the second taking over later where the current, and thus ν/γ , reaches a maximum; thus in Fig. 6 the anode damage and pinhole photograph show only annular distribution on a SPLATTLET shot in which tube envelope breakdown ended the pulse prematurely. Moreover the proportional contribution to the second mode of current is observed to be greater with the SPLATTLET duration of 100 ns than with MINI 'B's 50 ns, and greater in MINI 'B' shots for the higher currents.

The 'paraxial' component of emission is observed on MINI 'B' to converge to an extent dependent on ν/γ (or at least, current). Pinhole photographs and target damage using an axial target behind a foil window anode locate a focus 2 to

2.5 cm behind the anode under high vacuum conditions (p ~ 0.3 μ), not inconsistent with a convergence focus of the 'paraxial' component. Estimated beam trajectories are marked in Figs. 3 and 4; the circle denotes the size of the hole blown in a 0.003 in. thick tantalum target lying in a plane containing the axis of the tube. The trajectory marked with a query refers to the 'convergent' component of current; it is not yet clear what mechanism encourages such a path, indeed whether the electron trajectories arrive at the anode plane close to and parallel to the axis or whether they oscillate about the axis and propagate axially by drifting. Some evidence on this may arise when it becomes possible to determine the energy deposition profile in a target, and thus infer the mean angle of incidence of the beam electrons. Evidence that the annular 'paraxial' component converges strongly as shown and that its incidence on a target placed on focus is oblique, is given by the blow off of a shallow scab (~ 1 mm) of carbon from a calorimeter on focus at a total deposited energy of approximately 4.5 kJ. Later in SPLATTLET, with the larger annular cathode and under conditions producing a larger proportion of central core current, a much deeper scab (2-3 mm) was produced in the calirometer for a total energy less than 3 kJ; a small point lending weight to the hypothesis that the 'convergent' component does not oscillate, and has near-normal incidence to the target.

2.4 Multispot honeycomb cathode

The multispot configuration results from attempts to design a cathode (a) with large edge/area ratio; (b) with the facility for indefinite extension to cover any area; (c) with an easily recognisable pattern to facilitate the use of pinhole diagnostics.

Fig. 7 shows the type of cathode tested, mostly using the MINI 'B' generator. It comprises 19 spots of honeycomb material, each 1.02 cm in diameter by approximately 1 cm depth, arranged in a spot-centred hexagonal array of 2 cm pitch and flush inset into an aluminium electrode face. An earlier design of cathode consisted of 29 spots of plain Lucite each 1.02 by 1.0 cm in an asymmetric hexagonal array of 1.5 cm pitch; pinhole photos of the electron distribution incident on a tantalum anode for both types are shown in Fig. 7 for comparison. Emission is reasonably uniform, i.e. (a) each spot contributes a roughly equal fraction of the total current, and (b) in the case of the honeycomb version the shape and distribution of emission over each spot area is free of perturbations in the form of spots or striae, such as are visible in the case of the plain Lucite spots. Perveance is higher than any other cathode type and is consistent shot to shot; a few shots using SPLATTLET show a large dR/dt throughout the 100 ns pulse, the range of impedance straddling the value on MINI 'B' and extending over a factor of about five.

Conclusion (a) above ignores the presence on nearly all MINI 'B' shots of a near-central core, identifiable as possibly the 'convergent' component of current noted with the annular cathodes; the core, which is not very consistently central, is associated with heavy anode damage and presumably develops late in the pulse, or perhaps in subsequent pulses. Also, as with the annular cathode, the paraxial emission from the spot array is slightly convergent; the contraction in size of the 9 cm diameter pattern of the 19 spot array over a cathode-to-anode throw of 1.5 cm is about 5%, at a ν/γ of ~ 2.2. The pinhole data shows well defined spots, with no sign of smearing, due perhaps to radial movement, both in the case of MINI 'B' shots and those on SPLATTLET; the damage marks on anode or target, however, do show radially inward smearing. Since the radiation to which the pinhole camera is sensitive depends strongly on tube voltage (approx. $\alpha V^{2.5}$) the pinhole image is mainly laid down towards the end of the generator pulse where both voltage and current are at a maximum; such inward collapse of the emission pattern as is suggested by the smearing of anode damage marks is therefore presumed to take place either during the trailing decay of the pulse and/or during any subsequent reflections.

2.5 Cathode perveance

Fig. 8 summarises diode performance for the range of cathodes tested in the $\nu/\gamma > 1$ region, expressing performance in terms of normalised impedance as a function of electrode separation.

3. Beam Transport

Work on the transport of $\nu/\gamma > 1$ beams beyond the anode has been carried out so far only on a very limited scale; as a first step directed towards rapidly producing an energy deposition system, an extension of the annular cathode development was employed in which the current emerged through a 0.001 in. aluminium foil anode to form a focal spot about 2 cm in diameter at about 2.5 cm behind the anode. The ambient pressure in the diode and between anode and target was about 0.2 micron. It was found that the focal spot was more consistently kept centrally on axis if a 0.0002 in. thick aluminium foil was placed across the drift tube immediately in front of the target, which was usually a carbon calorimeter block. It was surmised that this foil was necessary to ensure a good low inductance return current path to the outer drift tube. Efficiency of energy transfer in most of these shots was close to 100%; maximum energy deposited was 5 kjoules.

3.1 Beam drifting

Only a few attempts have so far been made to propagate a beam in the 'drifting' mode, i.e. where the number density of slow electrons born in ionisation along the beam path is so high that their drift velocity back towards the anode window constitutes a current sufficient to cancel the self-magnetic field of the primary beam electrons. Under these conditions there are theoretically no radial forces acting on the beam, which drifts along, retaining its initial trajectories, and the 'return current' is carried within the beam by slow electrons, there being no need for an external drift tube to act as return current carrier. About 18 shots have been fired on MINI 'B' using a multispot honeycomb cathode as a launcher, as in Fig. 10, with a 0.001 inch aluminium window anode and a 0.003 inch tantalum target about 12 inches beyond the anode. The diode pressure was 0.1-0.3 μ, and that in the drift section varied between 0.1 and 20 torr. Figs. 9 and 10 show some typical open-shutter photographs of the drift section; those in Fig. 10 are taken in colour using a triple-lens camera with a different aperture on each lens.

Results were varied and inconsistent so far as the appearance of the beam is concerned; using integrated dose from the target as measured by thermoluminescent detectors as a parameter for comparison with the diode alone, the efficiency of transport of the beam was in most cases better than 30%, with a maximum of around 80%, with drift pressure between 0.5 and 1 torr.

Points of interest noted from these few shots were:

(a) Dendrite patterns in the Lucite drift tube, confined to the end near the target, and assumed to be caused by large currents of electrons reflected obliquely from the target.

(b) Apparent continuation of part of the beam beyond the target in some shots (see Fig. 10); this effect, together with (a) above, lend some support to the argument that the beam could contain a large fraction of electrons whose trajectories oscillate transverse to the axis.

(c) Multiple striae in some beam photos (Fig. 10), not clearly correlated with the cathode spot pattern but presumably caused by the spot emission; attempts to discern the hexagonal pattern of the cathode in the beam, even with a short drifting distance of 2 inches, have so far failed.

(d) Spotty and uneven distribution of current incident on the target, as shown by the pinhole photographs. This is also variable and inconsistent; some shots produced what looked like a gentle focussing effect under identical conditions to those quoted in Fig. 10.

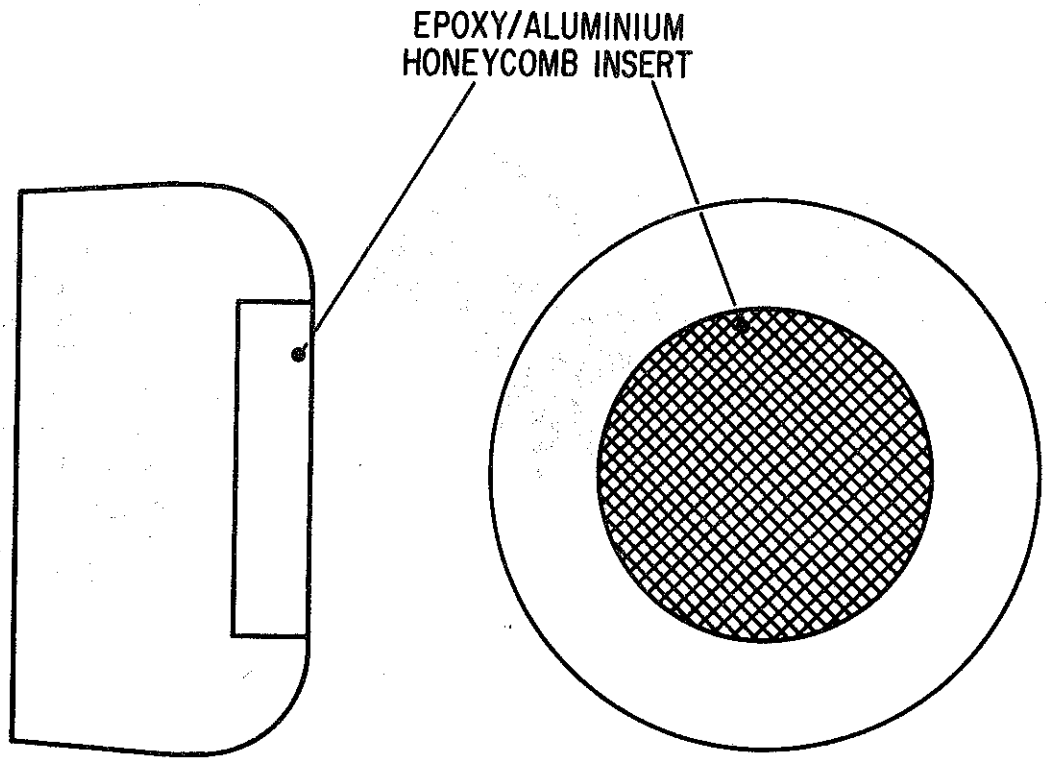

PITCH OF HONEYCOMB MESH ~ $\frac{1}{8}$ in

	CATHODE 1	CATHODE 2
O.D. OF ALUMINIUM ELECTRODE	3 in	7 in
O.D. OF HONEYCOMB INSERT	4.5 cm	9 cm
DEPTH OF INSERT	1 cm	1 cm

PLANE DISC HONEYCOMB PLASMA CATHODE

FIGURE 1

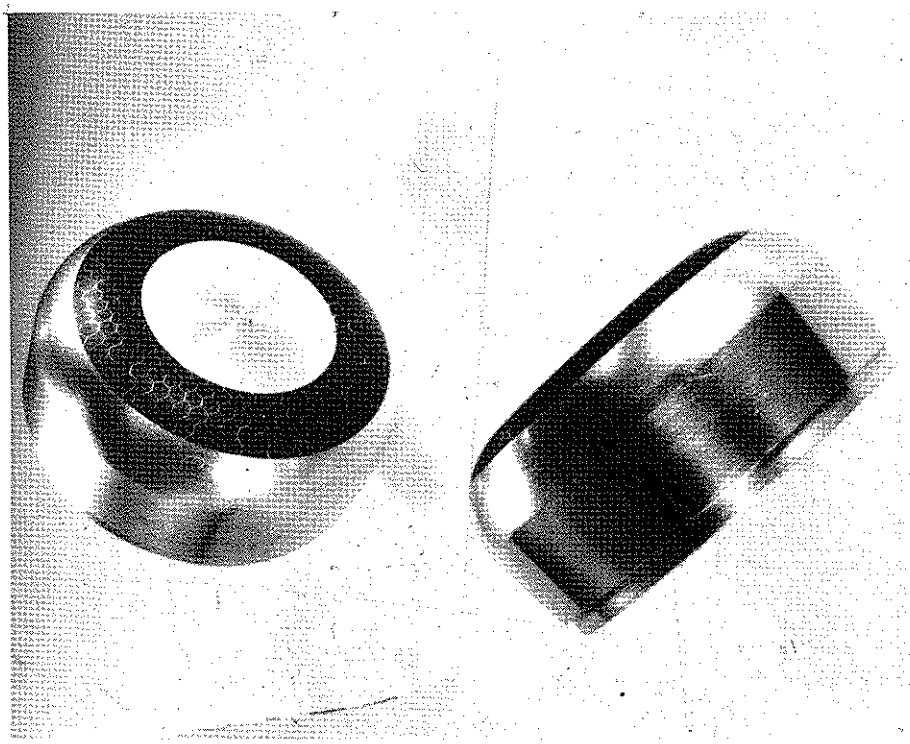

O.D. of honeycomb - 6.6 cm

I.D. of honeycomb - 4.0 cm

Depth of insert - 1.0 cm (at I.D.)

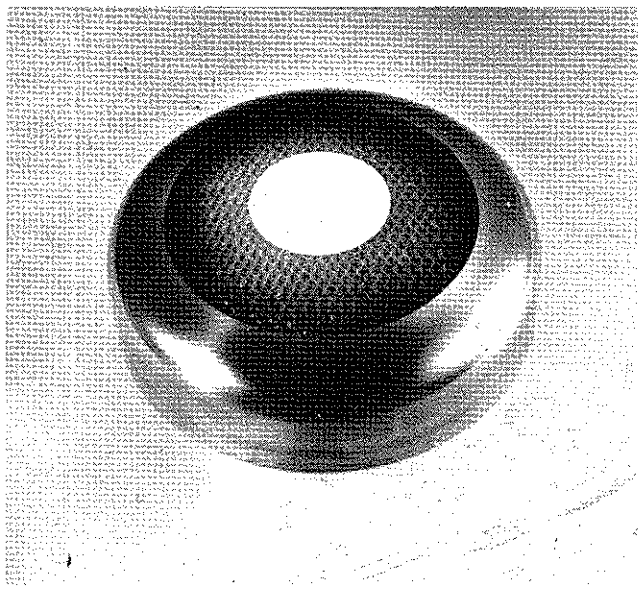

O.D. of honeycomb - 9 cm

I.D. of honeycomb - 4.0 cm

Depth of insert - 1.0 cm (at I.D.)

FIG. 2. ANNULAR HONEYCOMB PLASMA CATHODES

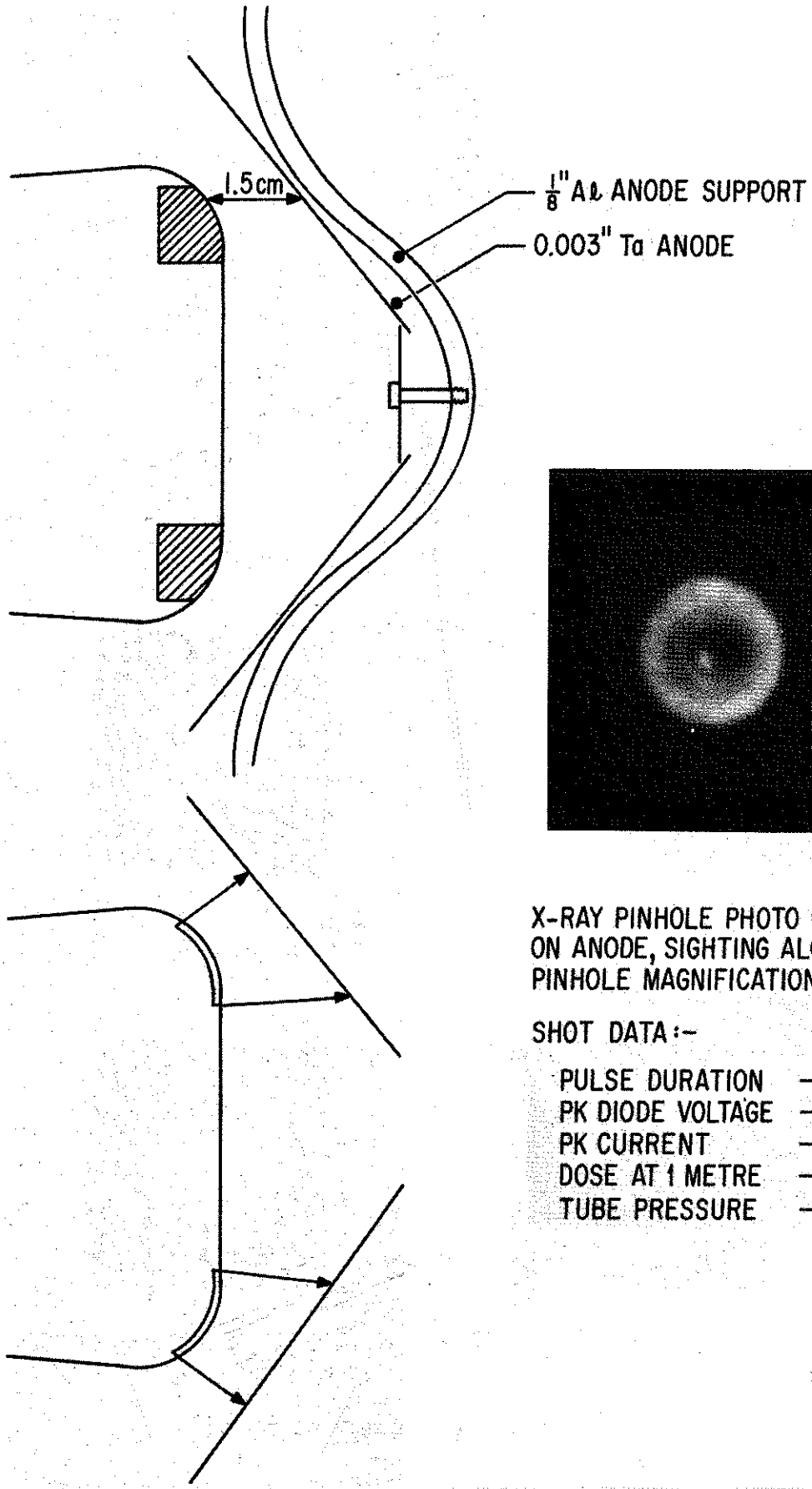

X-RAY PINHOLE PHOTO OF PATTERN ON ANODE, SIGHTING ALONG AXIS. PINHOLE MAGNIFICATION 3 TO 1.

SHOT DATA:–

PULSE DURATION	–	50 nsec
PK DIODE VOLTAGE	–	1.0 MV
PK CURRENT	–	90 kA
DOSE AT 1 METRE	–	1.2 r.
TUBE PRESSURE	–	0.3 μ

PINHOLE DATA AND BEAM TRAJECTORIES; SMALL ANNULUS; CONICAL ANODE GEOMETRY

FIGURE 3

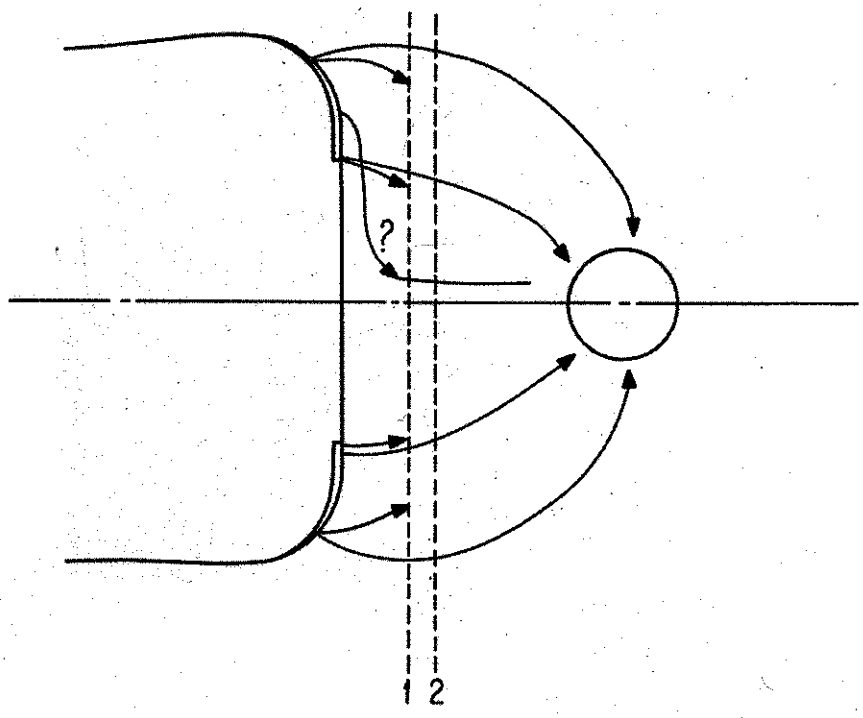

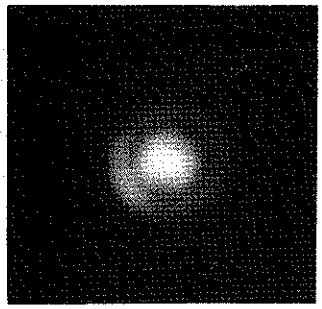

ANODE AT (1): A-K = 1.0 cm
Ipk = 100 kA; Vpk = 0.70 MV

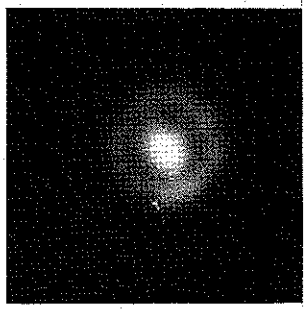

ANODE AT (2): A-K = 1.25 cm
Ipk = 80 kA; Vpk = 0.75 MV

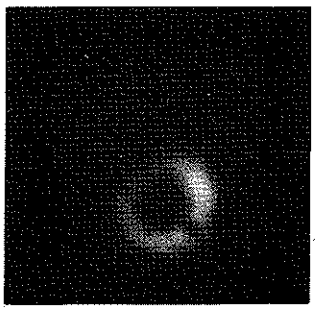

TARGET 1.0 cm BEHIND ANODE AT (2)
Ipk = 71 kA; Vpk = 1.0 MV

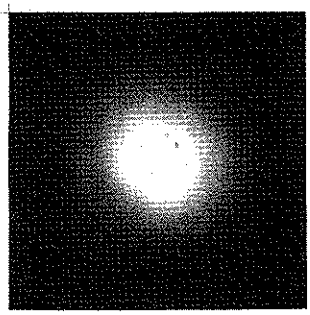

TARGET 2.5 cm BEHIND ANODE AT (2)
Ipk = 100 kA; Vpk = 1.4 MV

PINHOLE MINIFICATION - 3 TO 1.

PINHOLE DATA, BEAM TRAJECTORIES; SMALL ANNULUS; FLAT ANODE GEOMETRY

FIGURE 4

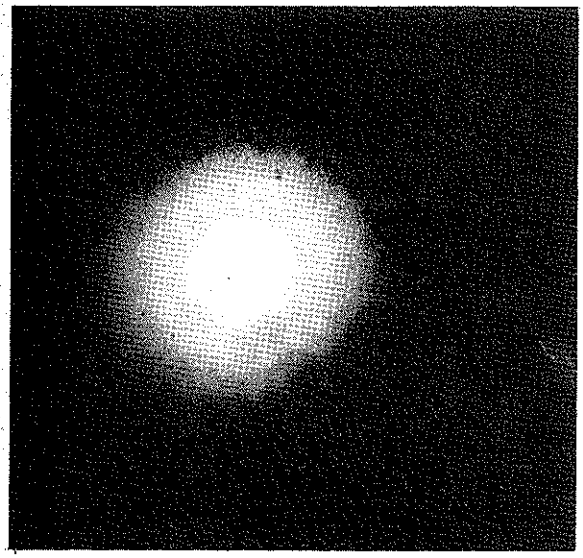

FIG. 5. PINHOLE PHOTO OF PATTERN FROM FLAT ANODE; LARGE ANNULUS IN SPLATTLET

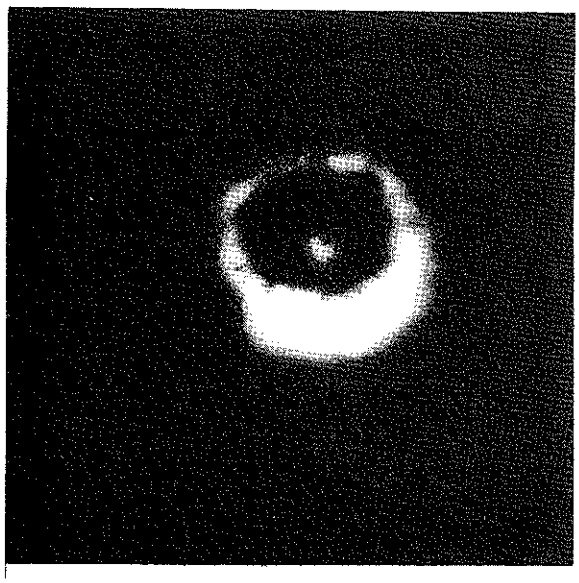

FIG. 6. PINHOLE PHOTO OF PATTERN FROM FLAT ANODE; LARGE ANNULUS IN SPLATTLET; SHORT PULSE

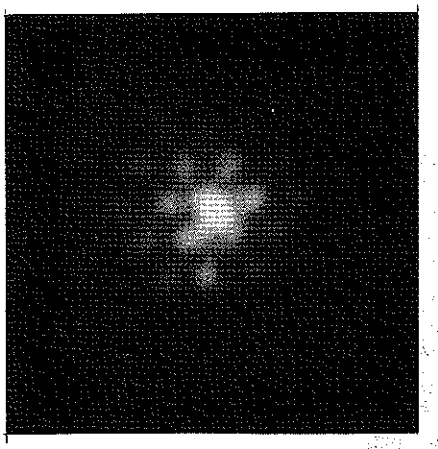

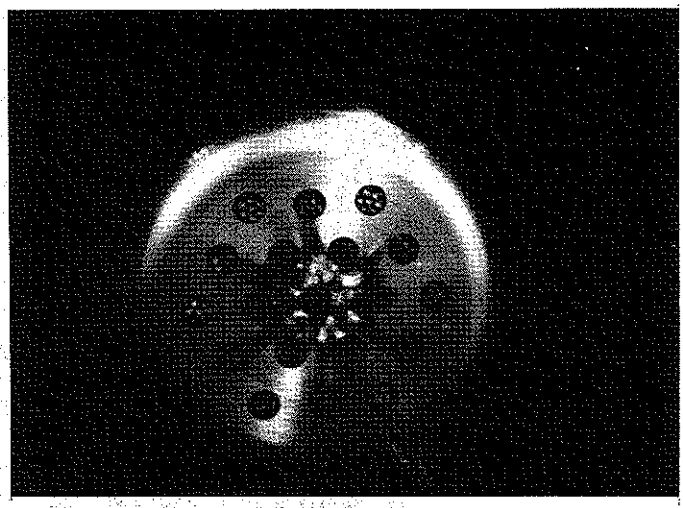

19-SPOT HONEYCOMB CATHODE;

Dia. of flat face - ~ 4"
" " inserts - 1.02 cm
Pitch " " 2.0 cm

Photo shows damage from blow up of tantalum anode 1.5 cms away.

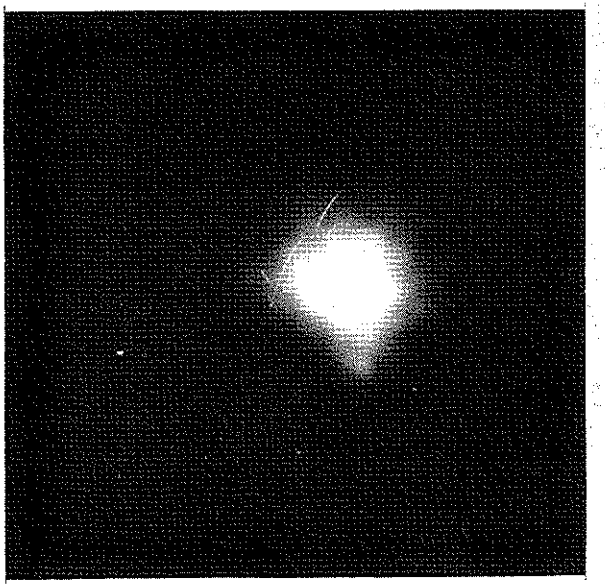

X-ray pinhole photos are of the cathode emission pattern from a Ta anode at 1.5 cms from cathode. Taken in MINI 'B' with
Ipk ~ 100 kA
Vpk ~ 1.0 MV.

29-SPOT LUCITE INSERT CATHODE;

Dia. of inserts - ~ 0.9 cm
Pitch " " - 1.5 cm

FIG. 7: MULTISPOT CATHODES

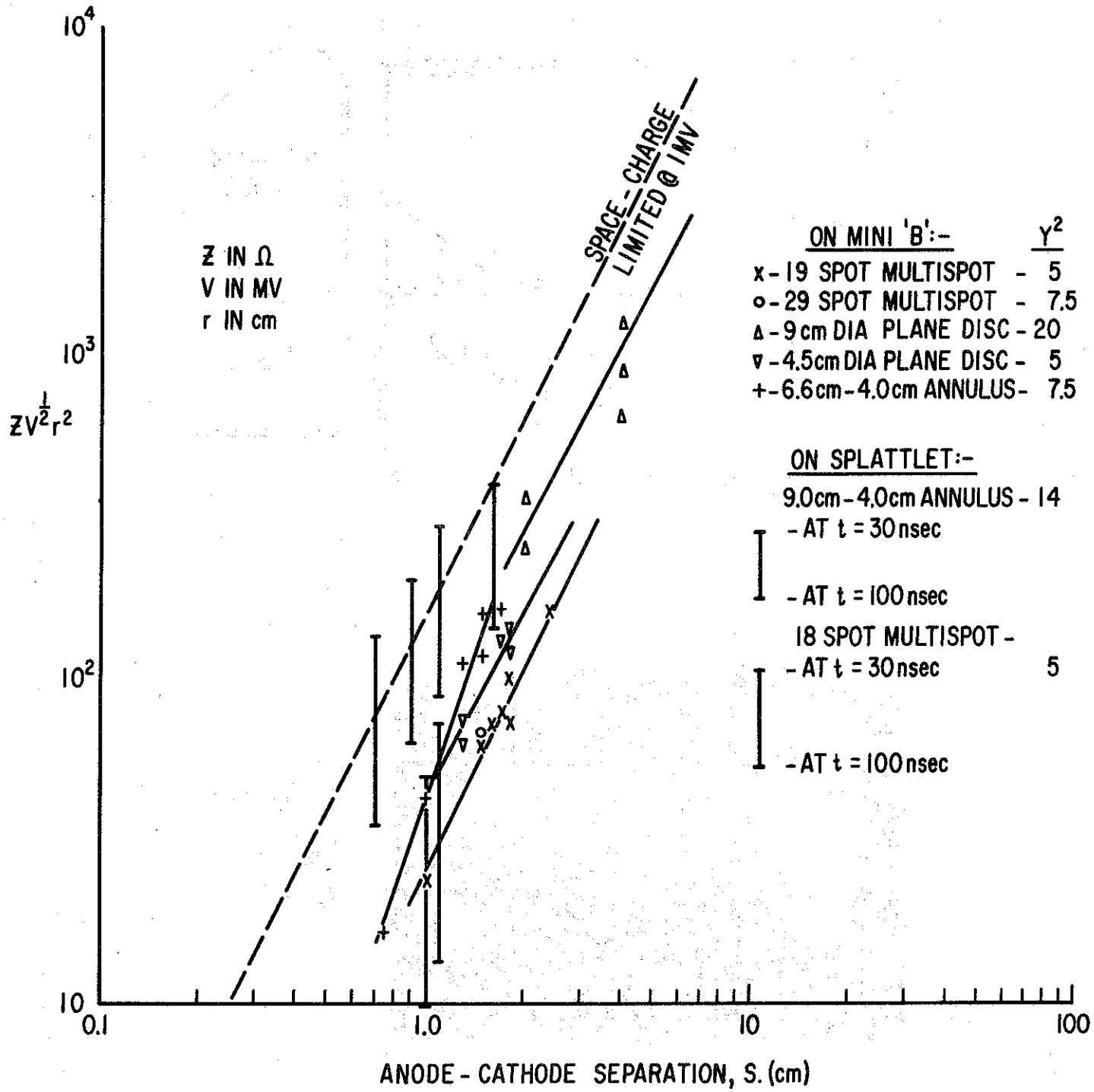
10^4
10^3
10^2
10
$ZV^{\frac{1}{2}}r^2$
Z IN Ω
V IN MV
r IN cm
SPACE-CHARGE LIMITED @ 1MV
ON MINI 'B':- Y^2
x - 19 SPOT MULTISPOT - 5
o - 29 SPOT MULTISPOT - 7.5
Δ - 9 cm DIA PLANE DISC - 20
▽ - 4.5cm DIA PLANE DISC - 5
+ - 6.6cm - 4.0cm ANNULUS - 7.5
ON SPLATTLET:-
9.0cm - 4.0cm ANNULUS - 14
- AT t = 30nsec
- AT t = 100nsec
18 SPOT MULTISPOT -
- AT t = 30nsec 5
- AT t = 100nsec
0.1
1.0
10
100
ANODE - CATHODE SEPARATION, S. (cm)

FIGURE 8

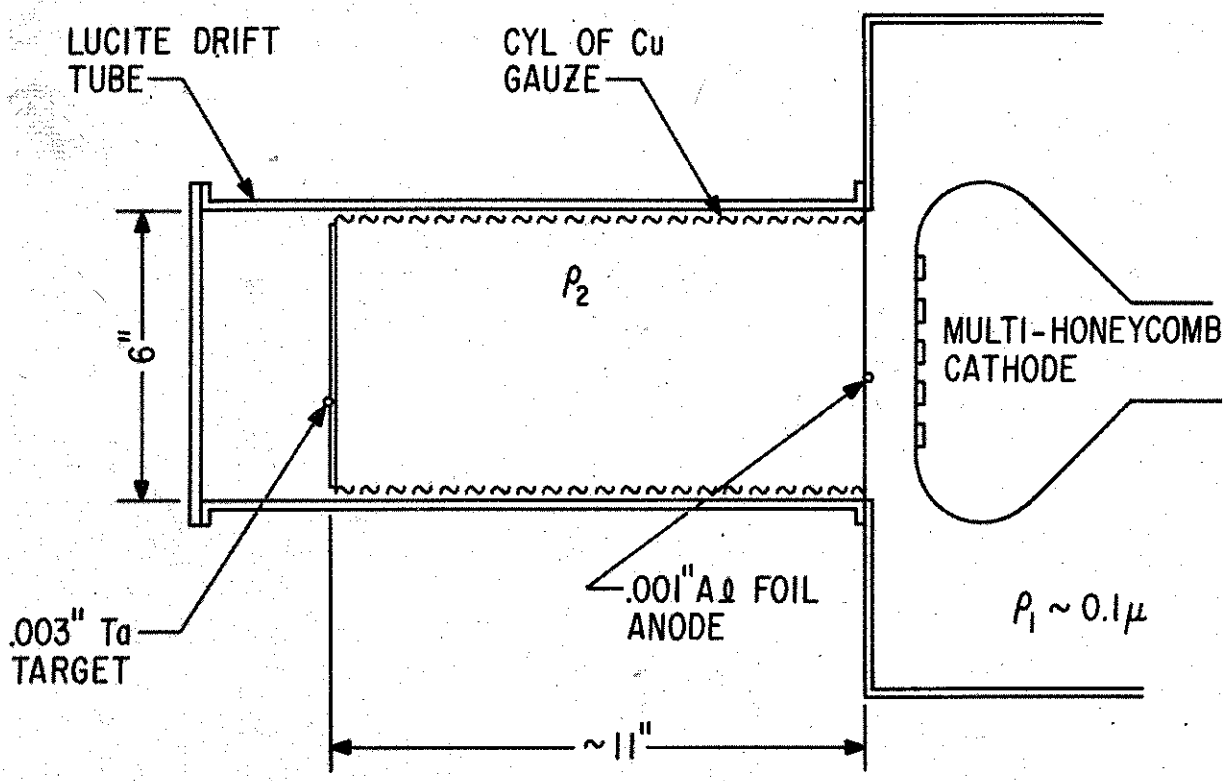

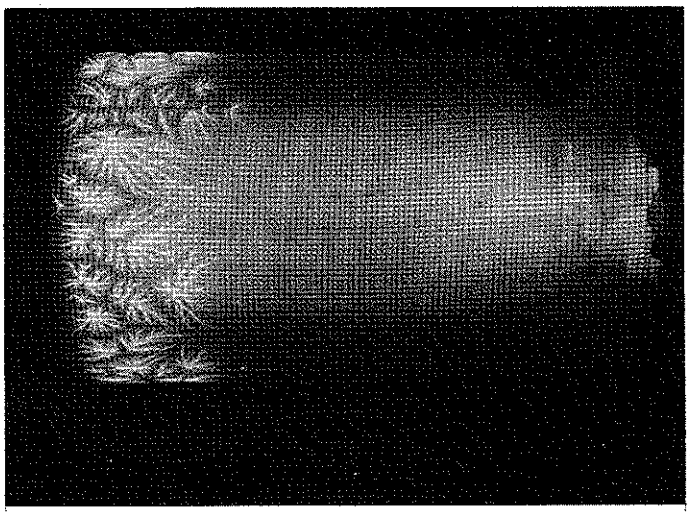

ρ_2 = 1.5 TORR
I_{PK} = 80KA
V_{PK} = 1 MV

FIGURE 9

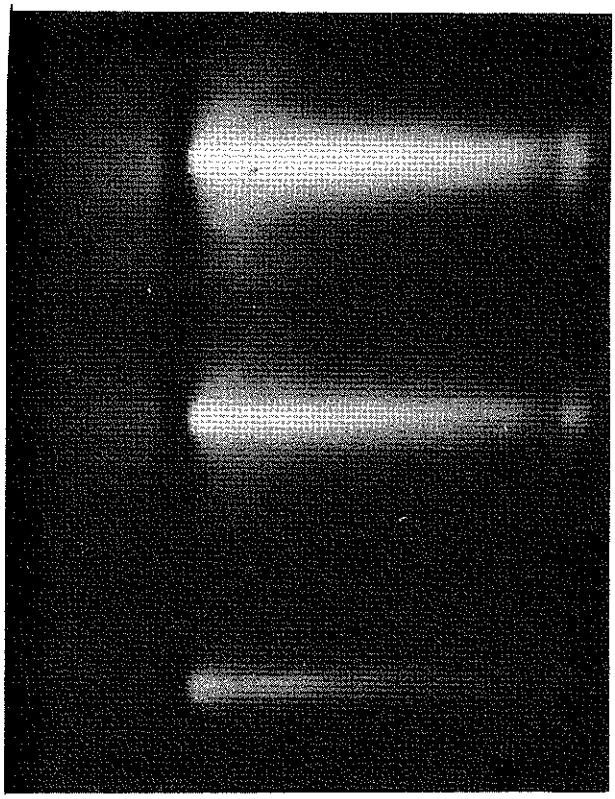

(Photo using triple-lens open shutter camera)

p_2 = 0.75 torr

Ipk = 80 kA

Vpk = 1.05 MV

Dose at 1 metre from target = 2.5 r

Pinhole photo of target pattern (minification 2.50:1)

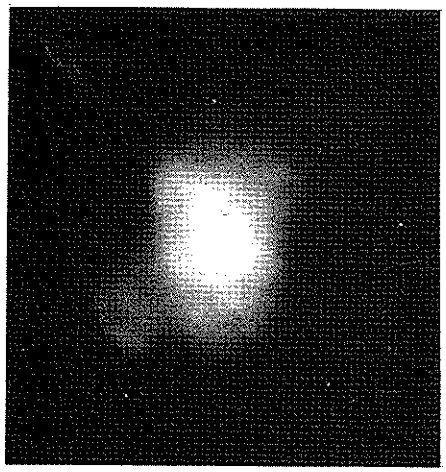

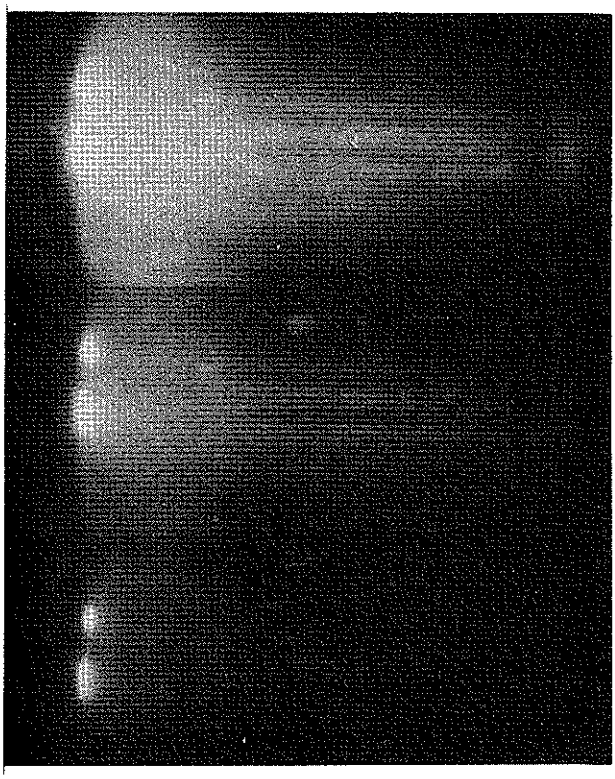

p_2 = 1 torr

Ipk = 70 kA

Vpk = 1.1 MV

Dose at 1 metre = 3.3 r.

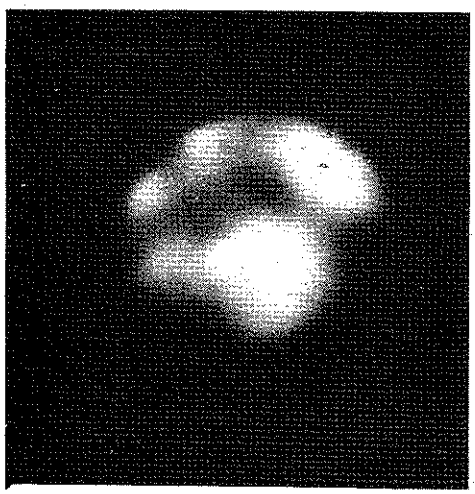

FIG. 10